IMPLEMENTATION OF UNBIASED FIR FILTERS WITH LOW-DEGREE POLYNOMIAL GAINS

Oscar Ibarra-Manzano[*], *Yuriy S. Shmaliy*[*], *Nasser Kehtarnavaz*[°], *Issa Panahi*[°], *Paula Castro-Tinttori*[*]

[*]Electronics Department, Guanajuato University
Ctra. Salamanca-Valle, 3.5+1.8km, Palo-Blanco, 36855, Salamanca, Mexico
phone: + 52 (464) 647-01-95, email: shmaliy@salamanca.ugto.mx, web: www.ingenierias.ugto.mx
[°]Department of Electrical Engineering, University of Texas at Dallas,
800 West Campbell Road, Richardson, Texas 75080, USA

ABSTRACT

We discuss implementation of the unbiased finite impulse response (FIR) filters. The transfer function and general block-diagram are presented for the l-degree polynomial FIR filter along with its fundamental properties in the z-transform domain. As a special results, we show a fundamental identity that is uniquely featured to such filters and can serve as an indicator of unbiasedness in filter design. For low-degree gains, the transfer function is represented in simple closed forms and compact block-diagrams. An example of applications is given for filtering of time errors in a crystal clock.

1. INTRODUCTION

Finite impulse response (FIR) estimators are commonly used whenever a linear phase response is required. Among known solutions, there is a special class of devices [1–3] intended for unbiased FIR filtering of oversampled signals. When such a filter is matched with the signal model, the group delay reaches a minimum. Otherwise, it grows with, however, lower rate than in the infinite impulse response (IIR) ones. The payment is a high order of FIR structures.

Simple implementation of FIR structures has become available after Heinonen and Neuvo designed the predictive FIR filters with polynomial gains [4]. These filters have been studied and used by many authors [5–9]. Later, Shmaliy showed in [10] that Heinonen-Neuvo's solution is unbiased and the theory of unbiased FIR estimators has been developed in [3, 10–13]. Most recently, in [14], it has been noticed that the unbiased FIR filter becomes virtually optimal when the number N of points in the average is large that makes it a useful engineering solution in optimal filtering.

Following [10], the unbiased FIR filtering estimate $\hat{x}_{n|n}$ of an l-degree polynomial signal x_n can be found in the convolution form at a current discrete time point n via measurement y_n obtained from $n-N+1$ to n as

$$\hat{x}_{n|n} = \sum_{i=0}^{N-1} h_{li} y_{n-i}\,, \tag{1}$$

where the l-degree polynomial FIR filter gain $h_{ln} \triangleq h_{ln}(N)$ is specified as

$$h_{ln} = \sum_{m=0}^{l} a_{ml} n^m \tag{2}$$

with the coefficient $a_{ml} \triangleq a_{ml}(N)$,

$$a_{ml} = (-1)^m \frac{M_{(m+1)1}}{|\mathbf{D}|}\,, \tag{3}$$

in which $|\mathbf{D}| \triangleq |\mathbf{D}(N)|$ is the determinant and $M_{(m+1)1} \triangleq M_{(m+1)1}(N)$ is the minor of the $(l+1)\times(l+1)$ quadratic matrix $\mathbf{D} \triangleq \mathbf{D}(N)$,

$$\mathbf{D} = \begin{bmatrix} d_0 & d_1 & \dots & d_l \\ d_1 & d_2 & \dots & d_{l+1} \\ \vdots & \vdots & \ddots & \vdots \\ d_l & d_{l+1} & \dots & d_{2l} \end{bmatrix}, \tag{4}$$

which generic component $d_v = \sum_{i=0}^{N-1} i^v$, $v \in [0, 2l]$, is determined by the Bernoulli polynomials (see Appendix A in [10]). The gain (2), existing from zero to $N-1$, has the following fundamental properties: the sum of its coefficients is unity, $\sum_{n=0}^{N-1} h_{ln} = 1$, and the moments are zeroth,

$$\sum_{n=0}^{N-1} h_{ln} n^u = 0\,, \quad 1 \leqslant u \leqslant l\,. \tag{5}$$

For low-degree polynomial signals, the unique ramp, quadratic, and cubic gains were originally found in [10–12] to be, respectively,

$$h_{1n} = \frac{2(2N-1)-6n}{N(N+1)}\,, \tag{6}$$

$$h_{2n} = \frac{3(3N^2-3N+2)-18(2N-1)n+30n^2}{N(N+1)(N+2)}\,, \tag{7}$$

$$h_{3n} = \frac{8(2N^3-3N^2+7N-3)-20(6N^2-6N+5)n+120(2N-1)n^2-140n^3}{N(N+1)(N+2)(N+3)}\,, \tag{8}$$

and higher degree gains can be found similarly.

Below, we consider design and application of the unbiased FIR filters with low-degree gains (6)–(8), by finding closed-form transfer functions and compact block-diagrams.

2. TRANSFER FUNCTION OF THE UNBIASED FIR FILTER

The transfer function of the discrete-time l-degree unbiased FIR filter is specialized with the z-transform applied to the

 ISSN 2076-1465

gain (2) as

$$H_l(z) = \sum_{n=0}^{N-1} h_{ln} z^{-n} \quad (9)$$

$$= \sum_{m=0}^{l} a_{lm} \sum_{n=0}^{N-1} n^m z^{-n}, \quad (10)$$

where $z = e^{j\omega T}$, ω is the angular frequency, T is the sampling time, and a_{lm} is specified with (3). The following properties of $H_l(z)$ can be listed in addition to the inherent ones of 2π-periodicity, symmetry of $|H_l(z)|$, and asymmetry of $\arg H_l(z)$.

2.1 Transfer Function at $k = 0$

By $\omega = 0$, we have $z = 1$ and, referring to (10) and (5), obtain

$$H_l(z) = 1 \quad (11)$$

for all l, meaning that the unbiased FIR filters is essentially an LP filter.

2.2 Filter Gain at $n = 0$

By the inverse z-transform, the value of h_{ln} at $n = 0$ becomes

$$h_{l0} = \frac{1}{2\pi j} \oint_{C_1} \frac{H_l(z)}{z} dz \quad (12a)$$

$$= \frac{1}{2\pi} \int_0^{2\pi} H_l(e^{j\omega T}) d(\omega T). \quad (12b)$$

Because h_{l0} is positive, $h_{l0} > 0$, for all l and $N \geqslant 2$ [10], the counterclockwise circular integration in (12a) always produces a positive imaginary value that gives us

$$\oint_{C_1} \frac{H_l(z)}{jz} dz = 2\pi h_{l0} > 0. \quad (13)$$

2.3 Transfer Function at $\omega T = \pi$

With $\omega T = \pi$, we have $z^{-n} = e^{-j\pi n} = (-1)^n$ and provide

$$H_l(z = e^{j\pi}) = -\sum_{m=0}^{l} \frac{a_{lm}}{2} \left[(-1)^N E_m(N) - E_m(0)\right], \quad (14)$$

where $E_m(x)$ is the Euler polynomial. For most widely used the low-degree gains, $0 \leqslant l \leqslant 3$, the Euler polynomials are given with $E_0(x) = 1$, $E_1(x) = x - \frac{1}{2}$, $E_2(x) = x^2 - x$, and $E_3(x) = x^3 - \frac{3}{2}x^2 + \frac{1}{4}$.

2.4 Energy

If $H_l(z)$ is the z transform of h_{ln}, then, by the Parceval theorem and (5), one has

$$\frac{1}{2\pi} \int_0^{2\pi} |H_l(e^{j\omega T})|^2 d(\omega T) = \sum_{n=0}^{N-1} h_{ln}^2$$

$$= \sum_{j=0}^{l} a_{jl} \sum_{i=0}^{N-1} h_{li} i^j$$

$$= a_{0l} = h_{l0}, \quad (15)$$

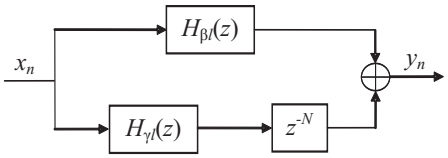

Figure 1: A generalized block-diagram of the l-degree unbiased FIR filter.

meaning that the gain energy in the transform domain is equal to the value of h_{ln} at $n = 0$. Comparing (15) and (13), one arrives at a noble identity

$$\int_0^{2\pi} H_l(e^{j\omega T}) d(\omega T) = \int_0^{2\pi} |H_l(e^{j\omega T})|^2 d(\omega T), \quad (16)$$

uniquely featured to the discrete-time unbiased FIR filters in the transform domain.

2.5 Noise power gain

The noise power gain (NPG) $g_l \triangleq g_l(N)$ is defined in [4] by the energy of h_{ln}, characterizing noise amount in the output of digital filters [15]. By Parceval's theorem and (16), the NPG can be evaluated in the following forms of

$$g_l = \frac{1}{2\pi} \int_0^{2\pi} |H_l(e^{j\omega T})|^2 d(\omega T) \quad (17a)$$

$$= \frac{1}{2\pi} \int_0^{2\pi} H_l(e^{j\omega T}) d(\omega T) \quad (17b)$$

$$= h_{l0} = a_{0l}. \quad (17c)$$

We notice that an analysis of g_l for $0 \leqslant l \leqslant 3$ in the time domain is given in [10].

3. TRANSFER FUNCTIONS OF LOW-DEGREE FIR FILTERS

Although the inner sum in (10) has no closed form for arbitrary m, it can be shown that the general form of $H_l(z)$ is

$$H_l(z) = \frac{\sum_{i=0}^{l} \beta_i z^{-i} + z^{-N} \sum_{i=0}^{l} \gamma_i z^{-i}}{1 + \sum_{i=1}^{l+1} \alpha_i z^{-i}}. \quad (18)$$

By assigning

$$H_{\beta l}(z) = \left(\sum_{i=0}^{l} \beta_i z^{-i}\right) \Big/ \left(1 + \sum_{i=1}^{l+1} \alpha_i z^{-i}\right), \quad (19)$$

$$H_{\gamma l}(z) = \left(\sum_{i=0}^{l} \gamma_i z^{-i}\right) \Big/ \left(1 + \sum_{i=1}^{l+1} \alpha_i z^{-i}\right), \quad (20)$$

we go to the generalized block-diagram of the l-degree unbiased FIR filter shown in Fig. 1. For low-degree gains, $0 \leqslant l \leqslant 3$, the coefficients in (18) are listed in Table 1, where a_{0l} can be defined by letting $n = 0$ in (6)–(8). That allows us to find the low-complexity block-diagrams for practical design of such filters with the ramp, quadratic, and cubic gains.

Table 1: Transfer Function Coefficients of the Low-Degree Unbiased FIR Filters

	l			
	0	1	2	3
β_0	$\frac{1}{N}$	a_{01}	a_{02}	a_{03}
β_1	0	$-\frac{4}{N}$	$-\frac{18(N-1)}{N(N+1)}$	$-\frac{48(N^2-2N+2)}{N(N+1)(N+2)}$
β_2	0	0	$\frac{9}{N}$	$\frac{24(2N-3)}{N(N+1)}$
β_3	0	0	0	$-\frac{16}{N}$
γ_0	$-\frac{1}{N}$	$\frac{2}{N}$	$-\frac{3}{N}$	$\frac{4}{N}$
γ_1	0	$-\frac{2(N-2)}{N(N+1)}$	$\frac{6(N-3)}{N(N+1)}$	$-\frac{12(N-4)}{N(N+1)}$
γ_2	0	0	$-\frac{3(N-2)(N-3)}{N(N+1)(N+2)}$	$\frac{12(N-3)(N-4)}{N(N+1)(N+2)}$
γ_3	0	0	0	$-\frac{4(N-2)(N-3)(N-4)}{N(N+1)(N+2)(N+3)}$
α_1	-1	-2	-3	-4
α_2	0	1	3	6
α_3	0	0	-1	-4
α_4	0	0	0	1

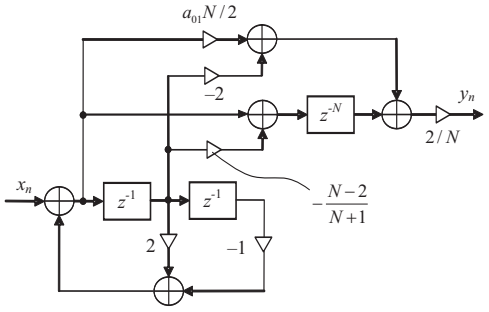

Figure 2: Block-diagram of the ramp unbiased FIR filter.

3.1 Ramp Gain

The transfer function for the ramp FIR filter, $l = 1$, can be found in the following compact form, if to use Table 1 and provide the transformations in (18),

$$H_1(z) = \frac{2}{N}\,\frac{\frac{a_{01}N}{2} - 2z^{-1} + z^{-N}\left(1 - \frac{N-2}{N+1}z^{-1}\right)}{(1-z^{-1})^2}. \qquad (21)$$

A simple analysis shows that the region of convergence (ROC) in (21) is for all z and that the filter is both stable and causal. Fig. 2 sketches the relevant block-diagram, which structure is N-invariant, utilizing 6 multipliers, 4 adders, and 3 time-delays. The magnitude and phase responses of the ramp unbiased FIR filter, case $l = 1$, are illustrated in Fig. 3 and Fig. 4, respectively. Figure 3a assures us that the unbiasedness is achieved by shifting and elevating the side lobes of the uniform FIR filter, $l = 0$. The phase response of this filter is linear in average (Fig. 4a). However, its function oscillates, similarly to the predictive FIR filters [5–7], making the group delay also oscillating about a small constant value (Fig. 4b).

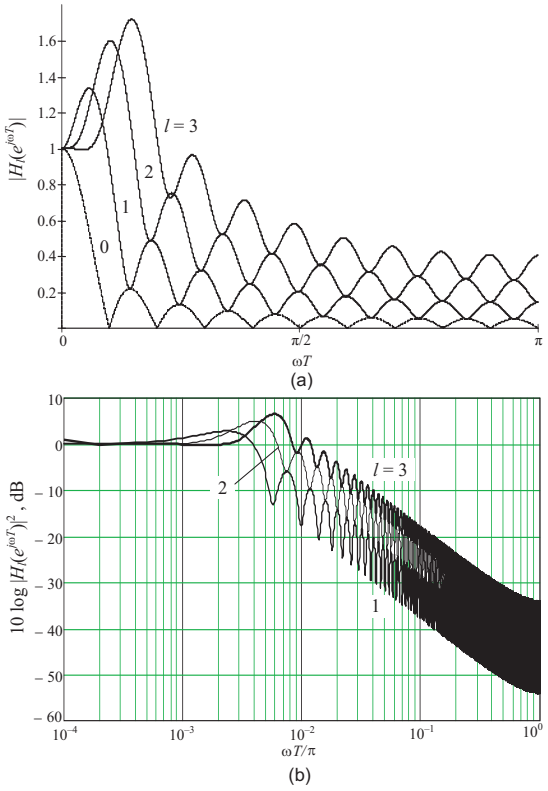

Figure 3: Magnitude response of the low-degree unbiased FIR filters: (a) $|H_l(e^{j\omega T})|$ for $N = 20$ and (b) Bode plot of $|H_l(e^{j\omega T})|^2$ in dB for $N = 500$.

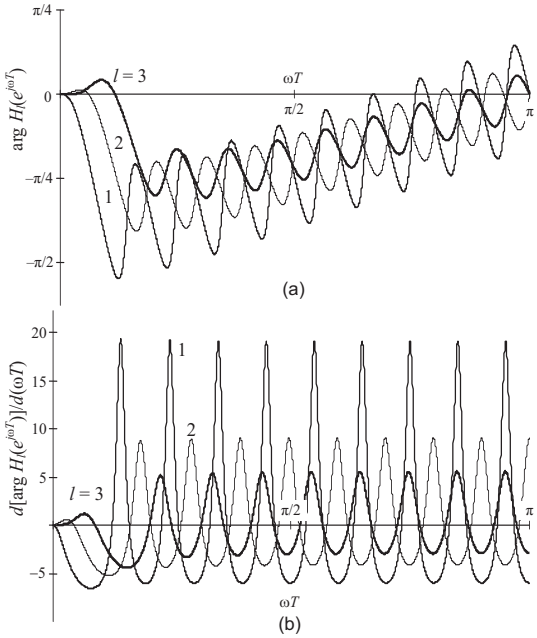

Figure 4: Phase characteristics of the low-degree unbiased FIR filters for $N = 20$: (a) phase response $\arg H_l(e^{j\omega T})$ and (b) group delay $d\,[\arg H_l(e^{j\omega T})]/d(\omega T)$.

$$H_2(z) = \frac{3}{N}\,\frac{\frac{a_{02}N}{3} - \frac{6(N-1)}{N+1}z^{-1} + 3z^{-2} - z^{-N}\left[1 - \frac{2(N-3)}{N+1}z^{-1} + \frac{(N-2)(N-3)}{(N+1)(N+2)}z^{-2}\right]}{(1-z^{-1})^3}. \tag{22}$$

$$H_3(z) = \frac{\frac{a_{03}N}{4} - \frac{12(N^2-2N+2)}{(N+1)(N+2)}z^{-1} + \frac{6(2N-3)}{N+1}z^{-2} - 4z^{-3} + z^{-N}\left(1 - b_1z^{-1} + b_2z^{-2} - b_3z^{-3}\right)}{N(1-z^{-1})^4/4}. \tag{23}$$

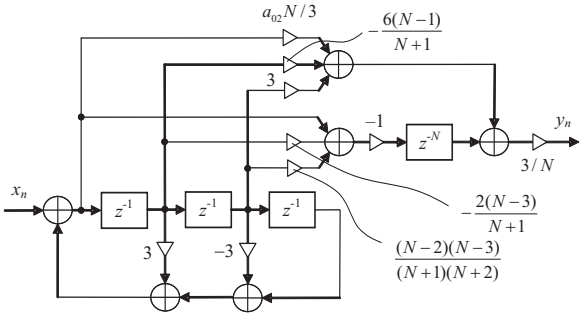

Figure 5: Block-diagram of the unbiased FIR filter with a quadratic gain.

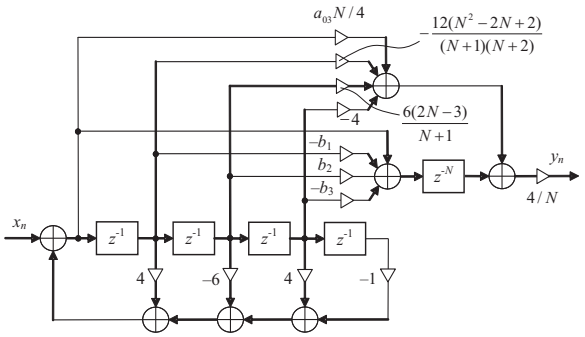

Figure 6: Block-diagram of the unbiased FIR filter with a cubic gain.

3.2 Quadratic Gain

After the routine transformations, the transfer function of the quadratic unbiased FIR filter becomes (22). The relevant block-diagram shown in Fig. 5 is performed with 9 multipliers, 5 adders, and 4 time-delays.

3.3 Cubic Gain

The unbiased FIR filter with a cubic gain, $l = 3$, can be represented with the transfer function (23), in which the coefficients are give by $b_1 = \frac{3(N-4)}{N+1}$, $b_2 = \frac{3(N-3)(N-4)}{(N+1)(N+2)}$, and $b_3 = \frac{(N-2)(N-3)(N-4)}{(N+1)(N+2)(N+3)}$. The block-diagram corresponding to (23) is sketched in Fig. 6. It is easily indicated that this filter requires 12 multipliers, 5 adders, and 4 time-shifters. The magnitude and phase responses of the filter with a cubic gain are given in Fig. 3 and Fig. 4. Observing these figures, one can trace an evolution of the filter transfer function, by increasing the filter degree.

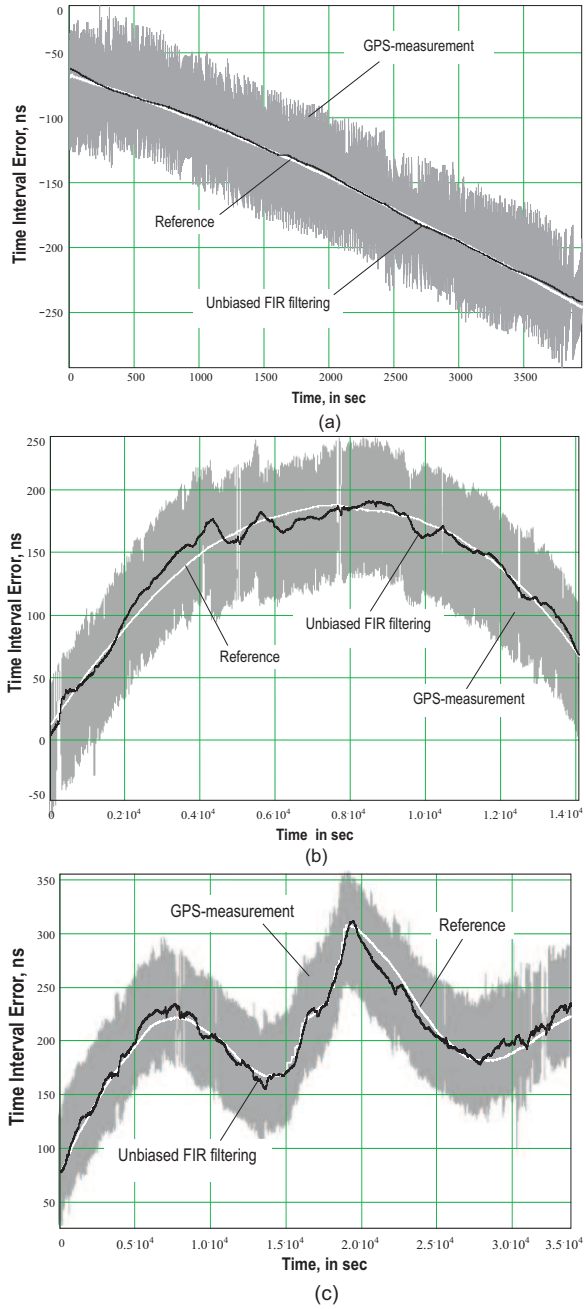

Figure 7: GPS-based unbiased FIR filtering of the crystal clock TIE: (a) near linear TIE behavior, (b) near quadratic TIE behavior, and (c) complex TIE behavior. Here "grey" plot represents the GPS-based measurement, "white" the reference trend, and "black" the estimate.

4. FILTERING OF CLOCK ERRORS

An experimental test of the unbiased FIR filters (Fig. 7) has been provided for the Global Positioning System (GPS)-based measurement of the time interval error (TIE) x_n of a precision crystal clock employing the one pulse per second (1PPS) signals of the SynPaQ III GPS Timing Sensor and Stanford Frequency Counter SR620 in the presence of the sawtooth noise induced in the receiver. To obtain the reference trend, the TIE has been simultaneously measured for the Symmetricom Frequency Cesium Standard CsIII employing another SR620. The clock was identified to have two states and the ramp FIR filter (Fig. 2) was therefore used.

In the first experiment, we selected a part of the process in which the TIE of the OCXO-based clock change with almost a constant linear slope. Following [18], the time step was set to be 1 s and the optimum N was experimentally found to be $N = 2060$. As can be inferred from the observation of Fig. 7a, the ramp FIR filter applied to the sawtooth measurement allows for the root mean square error (RMSE) of about 1.6 ns that is substantially lower than in the sawtooth corrected measurement [19].

For the second experiment, we selected a region where the TIE changed almost quadratically. In contrast to the near linear TIE trend (Fig. 7a), the optimum N has appeared here to be about $N = 920$. Numerical calculation gives us the RMSE of about 8.0 ns. Note that larger filtering errors are caused in Fig. 7b by the GPS time temporary uncertainties neatly seen in the GPS-based measurement and that there are no uncertainties in the reference measurement.

We finally exploit a part of measurement with a complex behavior of the TIE. The GPS-based and reference measurements and the estimate are shown in Fig. 7c. For this case, the optimum N was ascertained to be $N = 1150$ and the RMSE calculated as 7.83 ns.

5. CONCLUDING REMARKS

In this paper, we discussed the discrete-time l-degree polynomial unbiased FIR filter, its transfer function, and a generalized block-diagram. Fundamental properties of the filter transfer function have also been studied. A special attention has been paid to the most widely used low-degree gains (ramp, quadratic, and cubic), in which case the transfer function has been represented in simple closed forms and in compact block-diagrams. The magnitude and phase responses of the low-degree filters have been analyzed and compared to those of the predictive unbiased FIR ones. As an example of applications, we discussed filtering of the crystal clock errors via the GPS-based measurement of the TIE. It has been demonstrated graphically that the filter output has no time delay with respect to the reference trend.

REFERENCES

[1] E. Brookner, *Tracking and Kalman Filtering Made Easy,* John Wiley & Sons, New York, 1998.

[2] W. H. Kwon and S. Han, *Receding Horizon Control: Model Predictive Control for State Models,* Springer-Berlag, London, U.K., 2005.

[3] Y. S. Shmaliy, *GPS-Based Optimal FIR Filtering of Clock Models,* Nova Science Publ., New York, 2009.

[4] P. Heinonen and Y. Neuvo,"FIR-median hybrid filters with predictive FIR structures," *IEEE Trans. Acoust. Speech Signal Process.*, vol. 36, no. 6, pp. 892-899, Jun. 1988.

[5] J. Astola, P. Heinonen and Y. Neuvo,"Linear median hybrid filters," *IEEE Trans. Circuits and Systems*, vol. 36, no. 11, pp. 1430-1438, Nov. 1988.

[6] T. G. Campbell and Y. Neuvo, "Predictive FIR filters with low computational complexity," *IEEE Trans. Circuits Systems*, vol. 38, no. 9, pp. 1067-1071, Sept. 1991.

[7] S. J. Ovaska, O. Vainio, and T. I. Laakso, "Design of predictive IIR filters via feedback extension of FIR forward predictors," *IEEE Trans. Instrum. Measur.*, vol. 46, no. 5, pp. 1196-1201, Oct. 1997.

[8] X. Z. Gao, S. J. Ovaska, and X. Wang, "A fuzzy filter for sinusoidal signals with time-varying frequencies," *Int. J. Signal Process.*, vol. 1, no. 2, pp. 100-104, Apr. 2004.

[9] S. Samadi and A. Nishihara, "Explicit formula for predictive FIR filters and differentiators using Hahn orthogonal polynomials," *IEICE Trans. Fundamentals,* vol. E90-A, no. 8, pp. 1511–1518, Aug. 2007.

[10] Y. S. Shmaliy, "An unbiased FIR filter for TIE model of a local clock in applications to GPS-based timekeeping," *IEEE Trans. on Ultrason., Ferroel. and Freq. Contr.*, vol. 53, no. 5, pp. 862–870, May 2006.

[11] Y. S. Shmaliy, "A simple optimally unbiased MA filter for timekeeping," *IEEE Trans. on Ultrason., Ferroel. and Freq. Contr.*, vol. 49, no. 6, pp. 789–797, Jun 2002.

[12] Y. S. Shmaliy, "An unbiased p-step predictive FIR filter for a class of noise-free discrete-time models with independently observed states," in *Signal, Image, Video Process.,* vol. 3, no. 2, pp. 127-135, Jun. 2009.

[13] Y. S. Shmaliy, "Unbiased FIR filtering of discrete-time polynomial state-space models," *IEEE Trans. Signal Process.*, vol. 57, no. 4, pp. 1241–1249, 2009.

[14] Y. S. Shmaliy, "On real-time optimal FIR estimation of linear TIE models of local clocks," *IEEE Trans. on Ultrason., Ferroel. and Freq. Contr.*, vol. 54, no. 11, pp. 2403–2406, Nov. 2007.

[15] J. Ritzerfeld, "Noise gain expressions for low noise second-order digital filter structures," *IEEE Trans. Circuits Syst II, Exp. Briefs*, vol. 52, no. 4, pp. 223–227, Apr. 2009.

[16] D. Dang and W. Luo, "Color image noise removal algorithm utilizing hybrid vector filtering," *Int. J. Electron. Commun.*, vol. 62, no. 1, pp. 63–67, Jan. 2008.

[17] T. C. Ausal and K. E. Barner, "Hybrid polynomial filters for Gaussian and non Gaussian noise environment," *IEEE Trans. Signal Process.*, vol. 54, no. 12, pp. 4644–4661, Dec. 2006.

[18] Yu. S. Shmaliy, J. Munoz-Diaz, and L. Arceo-Miquel, "Optimal horizons for a one-parameter family of unbiased FIR filters," *Digital Signal Processing*, vol. 18, no. 5, pp. 739-750, Sep 2008.

[19] Yu. S. Shmaliy, O. Ibarra-Manzano, L. Arceo-Miquel, and J. Munoz-Diaz, "A thinning algorithm for GPS-based unbiased FIR estimation of a clock TIE model," *Measurement*, vol. 41, no. 5, pp. 538-550, June 2008.